JOURNAL OF MATERIALS SCIENCE 21 (1986) 217–224

Creep of chemically vapour deposited SiC fibres

JAMES A. DICARLO
National Aeronautics and Space Administration, Lewis Research Center, Cleveland, Ohio 44135, USA

The creep, thermal expansion, and elastic modulus properties for chemically vapour deposited SiC fibres were measured between 1000 and 1500° C. Creep strain was observed to increase logarithmically with time, monotonically with temperature, and linearly with tensile stress up to 600 MPa. The controlling activation energy was 480 ± 20 kJ mol^{-1}. Thermal pretreatments near 1200 and 1450° C were found to significantly reduce fibre creep. These results coupled with creep recovery observations indicate that below 1400° C fibre creep is anelastic with negligible plastic component. This allowed a simple predictive method to be developed for describing fibre total deformation as a function of time, temperature, and stress. Mechanistic analysis of the property data suggests that fibre creep is the result of β-SiC grain boundary sliding, controlled by a small percentage of free silicon in the grain boundaries.

1. Introduction

Substantial interest in continuous silicon carbide (SiC) fibres has developed recently because of their potential as reinforcement for high-temperature ceramic matrix composites. As a strong, stiff and thermally stable material, the SiC fibre should add not only strength and stiffness to a ceramic matrix but also improved fracture toughness. The mechanisms for toughening are many and strongly depend on the deformation and fracture properties of both composite constituents [1]. Thus the need arises for measuring and understanding the mechanical properties of SiC fibres, especially at high temperature where significant deviation from low-temperature behaviour can occur.

The primary objective of the present study was to determine the creep deformation behaviour of SiC fibres produced commercially by chemical vapour deposition (CVD). These fibres were chosen because in their as-produced state they offer significantly greater strength and modulus than continuous SiC fibres produced by other methods, such as polymer pyrolysis [2]. The experimental approach was to apply a constant axial load to a long-length fibre and then resistance-heat the fibre in an inert atmosphere at temperatures in the range 1000 to 1500° C. The advantages of this test approach were many. First, it allowed measurements of fibre creep strain as a function of time, temperature and stress. Second, the use of tensile stress and long fibre length simplified deformation analysis and permitted high-sensitivity strain measurements. Third, the resistance-heating method permitted direct and rapid temperature control and uniform temperatures along long fibre lengths. Last, but not least, the test method also allowed time-independent fibre thermal expansion and elastic modulus data to be obtained.

2. Experimental details

2.1. Specimens

The SiC fibre specimens were obtained commercially from Avco Specialty Materials Division, Lowell, Massachusetts. The basic fibre production method involved the chemical decomposition of a silane–hydrogen gas mixture on a resistivity-heated graphite-coated carbon monofilament which passed continuously through a CVD reactor [3]. For optimum fibre tensile strength, the decomposition temperature profile within the reactor decreased from ~ 1300° C at fibre entrance to ~ 1150° C at fibre exit.

The result of the SiC deposition is shown schematically in Fig. 1a. The filament cross-section displays an SiC sheath with an outer diameter of 142 μm surrounding an unreacted graphite-coated carbon core with an outer diameter of ~ 37 μm. The sheath microstructure consists of β-SiC columnar grains extending in the radial direction with ⟨1 1 1⟩ preferred orientation and lengths of a few micrometres [4]. At a radius of ~ 40 μm, a distinct change in microstrucure can be optically observed within the sheath. Associated with this change is an abrupt increase in average grain diameter from ~ 50 nm in the inner region (A) to ~ 100 nm in the outer region (B) [4]. This transition is the result of temperature and gas compositional differences from the entrance to the centre of the reactor.

Because of the deposition conditions, it was anticipated that the CVD SiC sheath should also contain small percentages of free silicon and carbon [5]. X-ray microprobe scans across the fibre cross-section showed that the silicon to carbon ratio increased in passing from Region A to Region B. This observation, coupled with the lower deposition temperature for Region B, suggests that this region contained free silicon. This conclusion is in agreement with the phase analysis results of Martineau *et al.* [6] who found that Region A generally contained a few per cent of excess carbon, whereas Region B was either stoichiometric or slightly silicon-rich.

To improve and maintain fibre strength, the manufacturer typically deposits thin silicon-containing carbon-rich coatings on to the SiC fibre surface.

0022–2461/86 $03.00 + .12

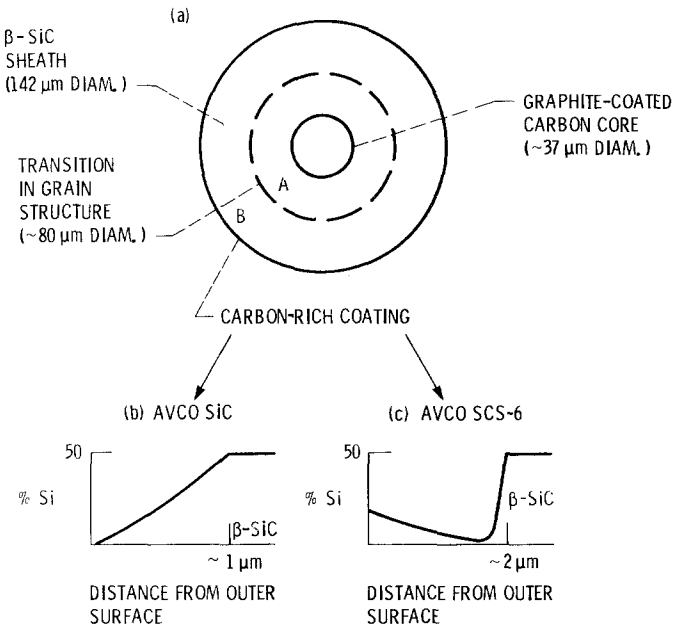

Figure 1 Schematic representations of (a) the CVD SiC fibre cross-section, and (b, c) the silicon content in the two types of carbon-rich fibre coatings.

Schematic representations of the silicon content in the coatings for the two fibre types employed in this study are shown in Figs. 1b and c. The coating for the standard SiC fibre (Fig. 1b) is graded in composition from amorphous carbon on the outside to approximately stoichiometric SiC at a depth of $\sim 1\,\mu m$ [7]. The $\sim 2\,\mu m$ thick coating for the SCS–6 fibre (Fig. 1c) consists of essentially pure amorphous carbon covered by a carbon-rich overlayer containing silicon in both the α- and β-SiC crystalline forms [4, 8]. Average as-received tensile strengths for the standard SiC and SCS–6 fibres in this study were 5.5 and 4.3 GPa respectively.

Although some fibre properties such as tensile strength can depend strongly on the carbon-rich coatings and the carbon core [9], fibre creep, thermal expansion and elastic modulus should be controlled only by the SiC sheath. That is, under axial deformation conditions, negligible stress should be carried by the coatings or core because their maximum volume fractions are only 3 and 7% respectively, and also because their moduli are significantly less than that of the SiC sheath. Indeed, the results of this study detected no deformation property differences between the standard SiC and SCS–6 fibres, even though their surface coatings were greatly different in microstructure and volume fraction.

2.2. Test procedure

The apparatus employed for the high-temperature deformation tests [10] is similar to a commercial CVD reactor in which a long length of fibre (~ 600 mm) is resistance-heated within a controlled gaseous environment. Water-cooled stainless steel caps at each end of a 25 mm diameter glass tube contain inlet and outlet gas ports and mercury seals for electrical contact with the fibre. Test runs were performed at 1 atm of nominally pure argon (0.01 vol % oxygen) flowing through the tube at $200\,cm^3\,min^{-1}$.

Axial tensile stresses were achieved by clamping the fibre above the top end-cap and adding various clamp loads below the lower cap. Travelling microscopes located at the clamps were used to measure deformations with an accuracy of $\pm 10\,\mu m$. Strain was calculated as the ratio of deformation to fibre length. For convenience, the applied tensile stress was calculated assuming the entire fibre cross-section carried the load. Thus listed stresses may underestimate the true sheath stresses by as much as 10%, assuming that coating and core carried no load.

Fibre temperature was determined at the fibre centre by optical pyrometer measurements corrected for fibre emmissivity, glass transmission losses and temperature gradients along the fibre. Average total emmissivity values calculated from electrical power input data were 0.66 and 0.75 for the standard SiC and SCS–6 fibres respectively. Temperature differences between the fibre center and the ends of the heated fibre section were small, reaching a maximum of 30° C at 1500° C. The error in the final temperature determination was estimated at $\pm 10°$ C. Above 1450° C, active oxidation effects [11] began to remove surface coatings and reduce fibre diameter. This problem limited test temperatures to a maximum of 1500° C.

For a typical test run, the initial procedure was to pretreat the fibre at a given temperature for 30 min. This was accomplished by clamping the fibre under minimal load (9 g) to achieve straightness and then increasing the d.c. current to a preset value which was held constant throughout the run. Thermal equilibrium conditions were attained in ~ 5 min, allowing accurate measurements of fibre thermal expansion.

Following the pretreatment run, loads ranging from 450 to 1000 g were applied at room temperature. The resulting deformation was used to determine the 20° C elastic modulus, E_0. Loads larger than 1000 g were attempted, but this usually resulted in fibre fracture either upon loading at room temperature or upon reaching test temperature. The sources of fracture were not examined. The fibre was then rapidly heated (~ 10 sec) to the same pretreatment temperature, where a time-dependent creep deformation was observed and measured. After 30 min or more, current was quickly (~ 10 sec) decreased to zero, leaving a

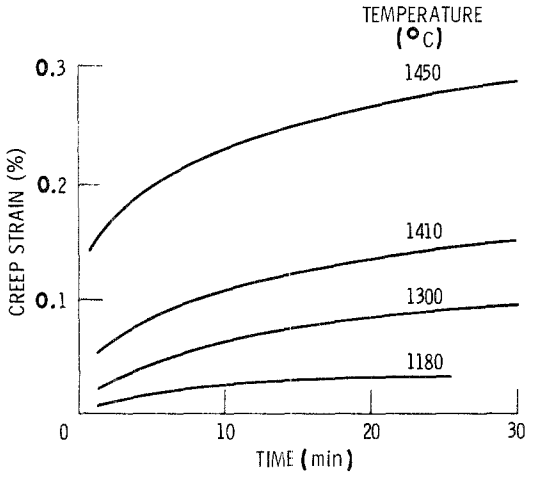

Figure 2 Typical creep data for CVD SiC fibres at a stress of 278 MPa.

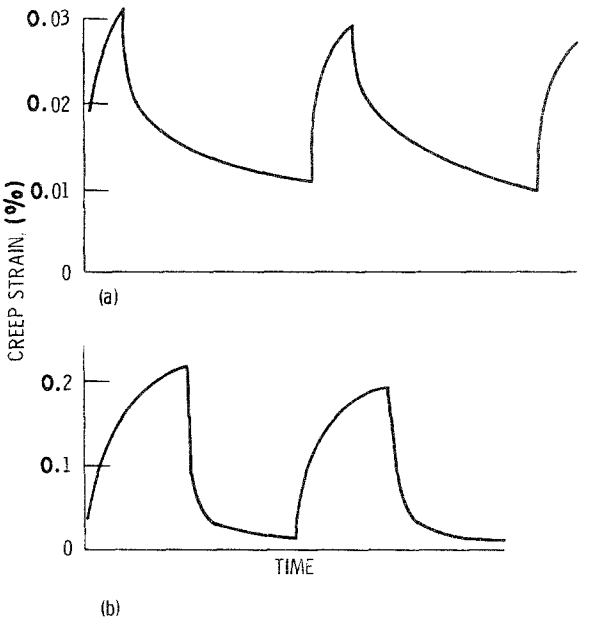

Figure 3 Creep and creep recovery curves for repeated load/no-load cycles. (a) Creep cycle 1180° C, 30 min, 278 MPa; recovery cycle 1180° C, 150 min. (b) Creep cycle 1275° C, 30 min, 612 MPa; recovery cycle 1450° C, 30 min.

residual creep strain in the fibre. The length change upon cooling was slightly larger (by ΔL) than the fibre expansion previously measured during the pretreatment run. This reflects a smaller fibre elastic modulus at the test temperature than at 20° C. The modulus ratio E/E_0 at temperature was calculated from

$$\frac{E}{E_0} = \left(1 + \frac{E_0 \Delta L}{\sigma L}\right)^{-1} \quad (1)$$

where σ is the applied stress and L the heated fibre length.

In some cases, creep runs were performed on as-received fibres with no preceding thermal pretreatment. Also, in a few instances, specimens with developed creep strains were reheated under minimal load (9 g) to the same or to a higher test temperature in order to measure creep recovery as a function of time. In some situations, creep and creep recovery tests were repeated two or three times on the same specimen.

3. Results

3.1. Creep

Typical fibre creep curves for various temperatures and a stress of 278 MPa are shown in Fig. 2. For time periods ranging up to a few hours, the creep curves were found to follow very nearly a logarithmic dependence on time. This indicates that the microstructural imperfections responsible for creep became limited in motion due to the buildup of internal stresses. If imperfection motion is reversible, then applied stress removal should allow the internal stresses to force the imperfections back to their original positions, provided the temperature is high enough to activate motion. As such, creep recovery would be observed and fibre deformation would be classified as anelastic or recoverable [12].

The fact that SiC fibre creep deformation is indeed anelastic is demonstrated by the creep and creep recovery curves of Fig. 3. Turning first to Fig. 3a, one finds that over 60% of the strain developed in 30 min at 1180° C and 278 MPa was recovered in 150 min at the same temperature and zero load. The trend of the curve suggests that further recovery would have occurred beyond 150 min, but the time required for almost complete recovery would have been considerably large. However, since creep is controlled by thermally-activated motion, recovery should be quicker if the recovery temperature is allowed to be greater than the test temperature. This fact is clearly shown by the curves of Fig. 3b where over 90% of the creep strain developed in 30 min at 1275° C was recovered in a similar time at 1450° C.

Besides demonstrating thermally activated creep recovery, the curves of Fig. 3 also show an interesting result concerning high-temperature mechanical fatigue of the fibres. For example, Fig. 3a indicates that at 1180° C, a tension–tension fatigue condition of 30 min with stress and 150 min without stress resulted in no cummulative increase in fibre creep strain. Indeed, residual strain actually decreased during cycling. A similar result is evident in Fig. 3b where the zero-load temperature was higher than the loading temperature. Certainly if the fibre creep strain contained any plastic or permanent deformation component, repeated cycling in the tension–tension mode should produce a net increase in strain. Thus it follows that at these stress and temperature conditions, CVD SiC fibre creep is entirely anelastic.

It should be made clear that the curves in Fig. 3 showing no increase in residual creep strain during cycling are a consequence of the recovery time–temperature cycle employed. Obviously, if the recovery cycle had a zero time duration, creep strain would continue to increase, following nearly a log(time) dependence.

Another important property characteristic of anelastic deformation is a linear dependence between creep strain ε_c and applied stress σ, or a creep compliance $J_c = \varepsilon_c/\sigma$ which is only time- and temperature-dependent and stress-independent. In order to demonstrate stress-independence for the fibre J_c, as well as to indicate the strong effects of thermal pretreatment on fibre creep, the creep compliance data

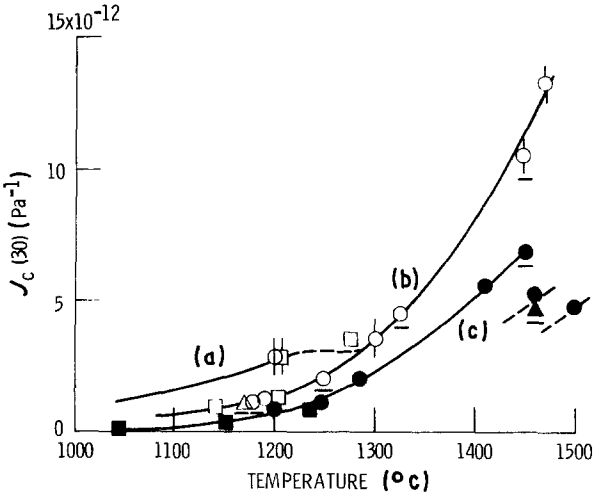

Figure 4 Temperature, stress and pretreatment dependence for the 30 min fibre creep compliance $J_c(30)$. Underlined data are for the SCS–6 fibres, stress (○, ●) 278 MPa; (△, ▲) 408 MPa; (□, ■) 612 MPa. Open symbols after 1150° C to 1360° C pretreatment; solid symbols after 1400° C to 1500° C pretreatment. Tailed symbols denote no pretreatments.

measured after 30 min, $J_c(30)$, were plotted in Fig. 4 as a function of test temperature. The applied stress levels and thermal pretreatment conditions are distinguished by the notation in the figure caption. Three pretreatment ranges are identified: 1150 to 1360° C, 1400 to 1500° C, and as-received or no thermal pretreatment. Data for the SCS–6 fibre are underlined.

Examining first the open symbols for pretreatment temperatures between 1150 and 1360° C, one finds that all the $J_c(30)$ data for the two fibre types fall very nearly on the same Curve (b). Since these data represent stresses ranging from 278 to 612 MPa, it follows that below 600 MPa, J_c is independent not only of fibre coating but also of stress. When the pretreatment temperature was increased above 1400° C, the solid data points show that a definite reduction in creep occurred across a wide temperature range. This dropoff further continued as pretreatment temperatures approached 1500° C. Apparently during pretreatment runs above 1400° C, microstructural changes occurred with the CVD fibre sheath which somehow reduced imperfection motion during the subsequent creep runs.

Finally, turning to the no pretreatment (tailed) data of Fig. 4, one finds two stress-independent points at 1200° C which are measurably greater than the Curve (b) data and three points above 1200° C which fall on Curve (b). (The Curve (a) extrapolation of the 1200° C data to lower temperatures will be explained shortly). These results suggest thermally-induced microstructural changes that reduce the creep also occurred between 1200 and 1300° C, as well as above 1400° C. That is, upon direct loading to 1200° C (or below), imperfections whose motion would otherwise be hindered by pretreatment runs near 1200° C were still available to participate in creep. Thus as-received creep up to 1200° C was greater than creep after pretreatment. However, upon direct loading to 1300° C and above, motion of these same imperfections became hindered because the 1200° C annealing temperature had been sufficiently exceeded. A similar argument can be used to explain why the as-received data above 1400° C were measurably higher than the 1400° C pretreatment data.

3.2. Creep analysis

The fact that time-dependent deformation below 1400° C can be classified as anelastic allows SiC fibre creep to be phenomenologically analysed and functionally described in terms of time, temperature and stress without any knowledge of the exact underlying physical mechanisms. This convenience is of practical significance, since it implies that fairly accurate predictions of total fibre deformation can be made for test conditions not included in the experimental data.

In anelastic theory [12], the total creep strain is the result of the cumulative motion of many small microstructural imperfections which move or relax at different times due to a distribution in relaxation times τ. Generally, as in the case for the SiC fibre, imperfection motion is thermally activated so that relaxation times decrease with increasing temperature according to the Arrhenius equation

$$\tau = \tau_0 \exp\left(\frac{Q}{RT}\right) \quad (2)$$

Here the activation energy Q is the height of the thermal barrier for relaxation, R is the gas constant, T is the absolute temperature and

$$\tau_0 = (2\pi\nu_0)^{-1} \quad (3)$$

where ν_0, the attempt frequency, is the number of times per second the relaxing imperfection attempts to cross the barrier.

The observation of logarithmic creep indicates that there are many relaxing imperfections participating in SiC fibre creep, and that the relaxation times are broadly distributed due to a broad distribution in τ_0 or Q or in both parameters. In this situation it is convenient to invoke the broad distribution approximation [12]. Under this approximation, an imperfection with relaxation time τ moves when $\tau = t$ so that by Equation 2

$$\ln t = \ln \tau_0 + \frac{Q}{RT} \quad (4)$$

To acertain whether the relaxation times were distributed in τ_0 or Q, the cross-cut method for determining activation energy Q was applied to the time-dependent creep curves measured in the 1150 to 1360° C pretreatment range. For this method, the log of the test time t required to achieve a certain strain level was plotted in Fig. 5 against the reciprocal test temperature. By Equation 4, the Q of the last imperfection to relax can be determined from the slope of the resulting straight line.

Examination of the best-fit lines of Fig. 5 shows that up to 1360° C, Q did not increase with creep strain but remained fairly constant at a value of 480 ± 20 kJ mol^{-1}. It can be assumed then that a broad distribution in τ_0 is the only source for the distribution in relaxation times. Letting $\gamma \equiv \ln \tau_0$, it follows by Equation 4 that creep strain observed at test temperature T after time t (sec) is the result of the cummulative

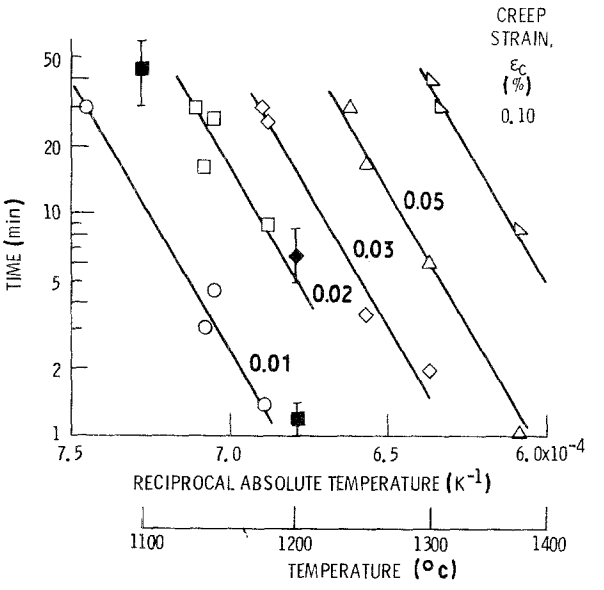

Figure 5 Time to reach various levels of fibre creep strain as a function of reciprocal absolute temperature (at 278 MPa stress). Solid points are from Marshall and Jones [20] for bulk siliconized SiC (at 303 MPa stress).

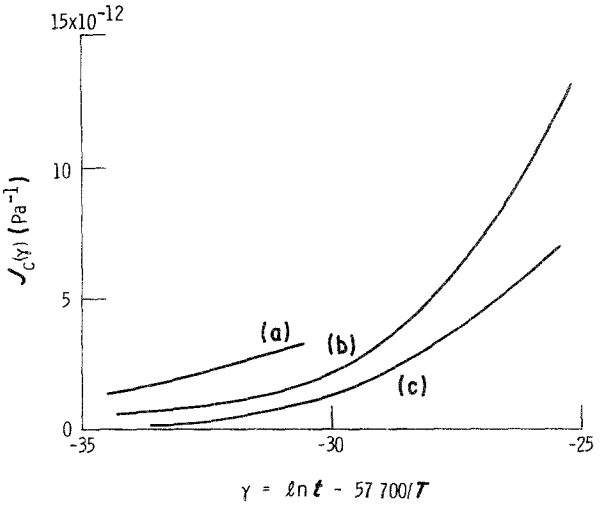

Figure 6 Functional dependence of the CVD SiC fibre creep compliance J_c on the relaxation parameter γ(t is in seconds and T in degrees Kelvin). (a) Pretreatment as-received up to 1150° C, test at < 1200° C. (b) Pretreatment as-received up to 1150° C, test at 1200° to 1450° C; also pretreatment 1150° to 1360° C, test at < 1450° C. (c) Pretreatment 1400° C to 1450° C, test at < 1450° C.

motion of imperfections with γ values equal to or less than

$$\gamma = \ln t - \frac{57\,700}{T} \quad (5)$$

Here Q/R has been replaced by the experimental value determined from Fig. 5.

In the light of the above analysis, fibre creep compliance J_c can be considered a function only of the relaxation parameter γ which is dependent on test time and temperature by the Equation 5 relationship. Thus if J_c is measured at a certain γ value, that same J_c will occur at any combination of time and temperature that gives the same γ value. It follows then that creep strain is predictable from

$$\varepsilon_c = \sigma J_c(\gamma) \quad (6)$$

where $J_c(\gamma)$ is an experimentally measurable function. To determine $J_c(\gamma)$ for the SiC fibre, the 30 min compliance results of Fig. 4 were employed to yield the three curves of Fig. 6. Curve (a) of Figs. 4 and 6 was constructed using Equation 6 and the short-time creep data for the as-received 1200° C specimens.

In conclusion, for temperatures below 1400° C and stresses below 600 MPa, the elastic and anelastic nature of CVD SiC fibre deformation allows one to make fairly accurate predictions of total fibre strain ε as a function of time, temperature and stress; i.e.

$$\varepsilon = \varepsilon_e + \varepsilon_c + \varepsilon_T = \frac{\sigma}{E} + \sigma J_c(\gamma) + \varepsilon_T \quad (7)$$

Here ε_e is the elastic strain component and ε_T the thermal expansion strain. It should be noted that for very long periods of time at constant temperature, $J_c(\gamma)$ varies slowly with time ($\sim t^{1/3}$) so that steady-state creep rates do not exist for the anelastic CVD SiC fibre, at least below 1400° C.

3.3. Thermal expansion

The thermal strain results for both types of CVD SiC fibre are given in Fig. 7. For warm-ups below 1350° C, strain increased in a nearly linear manner and was reproducible during cool-down. These data are in good agreement with the results of Kern *et al.* for bulk CVD SiC [13]. For warm-ups above 1360° C, however, the fibre thermal strain was observed to drop abruptly. As shown in Fig. 7, this contraction began near 1360° C and ended near 1390° C, amounting to an average strain decrease of 0.04%. Above 1400° C the thermal strain during warm-up followed a curve parallel to the extension of the lower-temperature curve.

On cool-down from above 1400° C, thermal strain followed the high-temperature warm-up curve until 1330° C, where it began to increase. At 1280° C this small expansion was complete and the cool-down curve followed the original low-temperature curve down to room temperature. A similar hysteretic effect was also observed by Kern *et al.* [13], who suggested free silicon as the source. This conclusion was based on the fact that on melting near 1400° C, silicon contracts when going from the solid to the liquid phase [14].

Careful monitoring of the fibre length at room temperature revealed a reproducible residual strain after the first thermal cycle above 1400° C. The 20° C tensile strain shown in Fig. 8 was measured after a 30 min

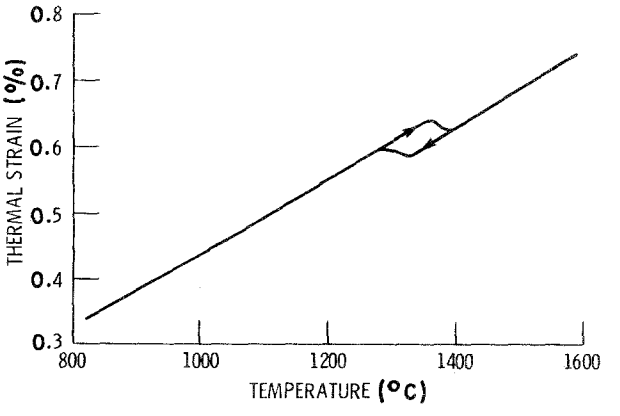

Figure 7 Thermal expansion strain for CVD SiC fibres.

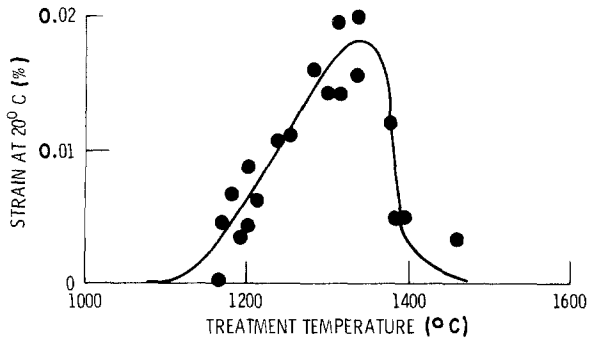

Figure 8 Residual strain in CVD SiC fibres observed at 20° C after 30 min thermal treatment and quenching from the indicated temperatures.

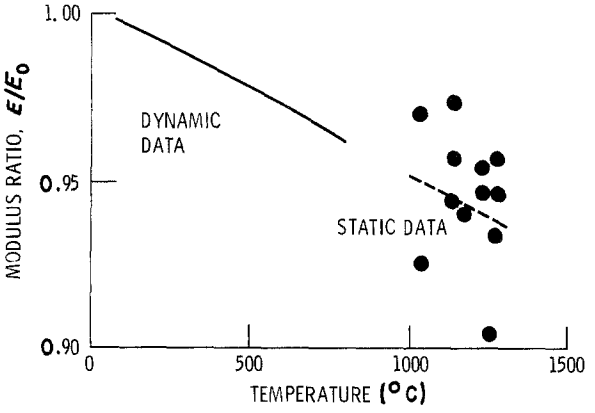

Figure 9 Temperature dependence for the elastic Young's modulus of CVD SiC fibres. $\bar{E}_0(20° C) = 391$ GPa.

thermal treatment at the indicated temperature, followed by a rapid quench to room temperature. From comparison with the Fig. 7 data, it can be concluded that this effect was probably caused by the contraction mechanism operating near 1400° C. That is, quenching the fibre after a 1400° C treatment resulted in a 20° C contraction which began to recover during thermal treatment near 1200° C. As the treatment temperature progressed above 1200° C, the recovery continued to occur until 1400° C where the contraction mechanism was allowed to operate again so that the entire process could be repeated.

3.4. Elastic modulus

The 20° C axial elastic modulus results for the standard SiC fibres are given in Table I. Included in this table are the moduli measured under static tension in this study and under dynamic flexure in a previous study [15]. The slight difference in modulus results is to be expected, since the tension method senses both the high-modulus SiC sheath and the low-modulus carbon core whereas the flexure method primarily senses the outer surface layers of the sheath. Accounting for the effects of core and coating for each test method [15], one can calculate sheath modulus values in fairly good agreement (Table I).

The temperature dependence of the elastic modulus of the standard SiC fibre is shown in Fig. 9. The high-temperature data points with large scatter were measured under static tension using Equation 1. The scatter arose from a lack of sufficient experimental resolution in length measurement ΔL rather than from real physical differences among the specimens. The more accurate low-temperature data shown by the continuous curve were measured previously using the sheath-sensitive dynamic flexure method [15].

4. Discussion

Because the CVD SiC fibre creep observed in this study is anelastic or recoverable and occurs at temperatures where dislocation motion is negligible [16], the controlling creep mechanism can be identified as grain boundary sliding (GBS) in which β-SiC grains under applied stress and high temperature move or slide with respect to their neighbours. Due to the buildup of elastic stresses at grain boundary intersections, the GBS process becomes limited in time, giving rise to creep saturation effects (see Fig. 2). When the applied stress is removed, the internal stresses force the grains to slide back to their original positions, resulting in macroscopic creep recovery.

TABLE I SiC fibre modulus at 20° C

Modulus	Fibre (measured, GPa)	Sheath (calculated,* GPa)
Axial static	391 ± 5	427 ± 5
Flexural dynamic	414 ± 9†	436 ± 9

*Using properties from DiCarlo and Williams [15].
†Taken from DiCarlo and Willaims [15].

Zener's theory for GBS [17] predicts that at the completion of grain motion, J_c for the SiC fibre should saturate at a value of 1.5×10^{-12} Pa^{-1}. Clearly the J_c results of Fig. 6 show much higher values with no evidence of saturation to at least 1450° C. Although there are many creep situations in which Zener's theory is indeed obeyed, there are also others in which experimental creep strains exceed his predictions [12]. As is the case for the CVD fibre, these large strains remain anelastic in that they are directly proportional to stress and can be recovered by stress removal.

One model that can be invoked to explain the large anelastic creep strains is that after simple motion of single grains as predicted by Zener, there can occur more complicated motion in which a set of multiple grains moves with respect to another set of multiple grains. Because the attempt frequency (see Equation 3) for multiple grain motion should be less than that for single-grain motion, the distribution for GBS creep should begin at the single-grain τ_0 and extend to larger and larger τ_0 for multiple-grain motion. In this regard, it is interesting to note that the ln τ_0 value typically observed for Zener single-grain motion is ln (10^{-15}) or -35, a value in good agreement with the γ in Fig. 6 where significant creep effects are first observed in the SiC fibre.

Turning to the mechanism controlling grain motion, it has been generally observed that for those creep situations with GBS as the accepted source, the activation energy controlling creep agrees closely either with the lattice self-diffusion energy or the grain-boundary self-diffustion energy of the particular material, or with the lattice self-diffustion energy of impurity phases in the grain boundaries. A physical

model for this correlation is that the viscosity of the interfacial boundary layer between grains is controlled by diffusion mechanisms in the layer [12]. Assuming this to be the case for the SiC fibre, one would then expect the measured creep activation energy of $480 \pm 20\,kJ\,mol^{-1}$ to possibly agree with the self-diffusion or grain-boundary diffusion energies of either silicon or carbon in polycrystalline β-SiC or with the self-diffusion energy of free silicon, since this metal (as discussed earlier) can exist to some degree within the CVD fibre. Comparing the literature values for these energies (Table II) with the creep energy of this study, one finds little agreement with the β-SiC values but excellent agreement with the silicon metal value. This observation suggests that β-SiC grain-boundary sliding in the CVD fibre is controlled by free silicon metal located within the grain boundaries.

Additional evidence for the presence of free silicon between β-SiC grains can be found in the decrease in thermal expansion strain observed near 1380° C during warm-up (see Fig. 7). As suggested by Kern *et al.* [13], this effect can be explained by the 9% reduction in volume [14] displayed by silicon metal when it changes from solid to liquid. Assuming that the observed fibre axial contraction of 0.04% occurred uniformly in all directions, and that the free silicon located between β-SiC grains contracted fully on melting, one estimates that V_{Si}, the average volume fraction of free silicon in the CVD fibre, is $\sim 1.4\%$. However, the large aspect ratio of the β-SiC grains and their preferred radial orientation suggests that silicon contraction should only be observed in the axial and tangential directions, so that a better estimate for V_{Si} under full contraction is $\sim 1\%$.

The 1% value for silicon content should be considered a lower limit because full silicon contraction was most likely prevented by internal constraints. Indeed, the difference between the normal-pressure silicon melting temperature (1410° C) and the temperature for contraction on warm-up (1380° C) and for expansion on cool-down ($\sim$ 1310° C) suggest by Clapeyron's equation that the excess silicon was under large internal compression (~ 1 GPa). Such high internal stress could have been generated by growth mechanisms during CVD [5] or possibly by the thermal expansion mismatch between the silicon and β-SiC.

At this point, one might compare the present creep results with literature data for other types of SiC ceramics at temperatures below 1500° C. This comparison is difficult in most cases because the creep data are usually presented in terms of "steady-state creep rates" which, as discussed earlier for anelastic creep, may actually be time-dependent. A more accurate comparison would be in terms of total creep strain measured under similar time, temperature and stress conditions. Such total creep strain measurements have been made by Marshall and Jones [20] for reaction-bonded or siliconized SiC (Refel) containing $\sim 10\%$ free silicon. As shown by the solid data points of Fig. 5, their results are in good agreement with the CVD fibre data. This close similarity in creep magnitude and activation energy is considered strong evidence for grain-boundary silicon as the controlling GBS phase for both types of SiC material. (The often-quoted activation energy of $230\,kJ\,mol^{-1}$ measured by Marshall and Jones [20] is believed to be incorrect due to their questionable energy-determination method).

TABLE II Activation energies for self-diffusion

Material	Lattice ($kJ\,mol^{-1}$)	Grain-boundary ($kJ\,mol^{-1}$)
β-SiC*: silicon	912 ± 5	–
carbon	841 ± 14	564 ± 9
Silicon metal†	494 ± 10	–
	460	–

*From Hon *et al.* [18].
†From Smithells and Brandes [19].

Regarding silicon-free sintered SiC ceramics, higher test temperatures are generally required to observe creep rates equivalent to those of siliconized SiC [21]. Since the sintered materials typically contain free carbon in the grain boundaries, these results suggest that GBS does occur in sintered SiC but, rather than silicon, carbon with its higher activation energy (see Table II) may be the creep-controlling intergranular phase.

Comparing CVD SiC fibre creep with that of the polymer-derived Nicalon SiC fibre [22], one finds almost an order of magnitude lower creep strain for the CVD fibre under similar test conditions. This can possibly be explained by the lower viscosity silicon-oxide phase known to be created in the Nicalon fibre during its production [2].

One final point that should be addressed is that of the possible sources for the creep reductions observed in the CVD fibre after thermal pretreatments near 1250 and 1450° C. In the light of the above GBS model, a reduction in creep could be explained by (i) a decrease in the number of grains available for sliding, or (ii) an increase in the viscosity of the grain-boundary material. Process (i) may typically occur by grain lock-up in which stress-driven motion during pretreatment places some grains in new locations where they are unable to move until applied stresses reach levels greater than those required for grain motion prior to pretreatment. Process (ii) may occur by the removal of the grain boundary material or by the addition of higher viscosity phases to the boundaries. Under this condition higher stresses should not be able to restore creep behaviour.

Because below 1400° C the free silicon remains intact within the grain boundaries, the 1250° C pretreatment effect was probably caused by Process (i). That is, under zero external load conditions, some of the grains moved to new positions where they became locked with respect to the maximum stress levels of this study (600 MPa). The internal diriving force for this grain motion was probably residual growth stresses in the outer sheath layers which were not fully relieved during the CVD process, because the time–temperature conditions during deposition were lower than those applied during pretreatment.

On the other hand, the 1450° C pretreatment effect occurred in a temperature region where effects from both Processes (i) and (ii) might be expected to operate. For example, internal stresses generated near 1400° C by the contraction effect might be expected to

move grains into new and possibly locked positions. Also, near 1450° C, free silicon in liquid form might be expected to diffuse rapidly and be removed from the boundaries, possibly by reaction with free carbon within the fibre sheath. As described above, the application of high stresses after pretreatment could clarify the responsible creep-reduction mechanism. However, at these temperatures there is a considerable loss in fibre tensile strength [9, 23] which significantly limits the applied stress. Thus, at the present time the mechanism for the 1450° C pretreatment effect remains uncertain. Nevertheless, the fact that this effect occurs near the silicon melting point is additional strong evidence for the presence of this metal in free form.

5. Concluding remarks

The deformation-property results of this study indicate that the sheath of the commercial CVD SiC fibre is a composite in itself, consisting of β-SiC grains with a small percentage of free silicon metal in the grain boundaries. Whereas the fibre modulus and thermal expansion strain are essentially controlled by the β-SiC grains, fibre creep below 1400° C appears to be the result of grain-boundary sliding controlled by the free silicon. As such, the CVD fibre displays creep characteristics similar to bulk SiC ceramics that are produced with excess silicon in their microstructure. Although fibre creep below 1400° C is greater than that of silicon-free SiC ceramics, its anelastic nature does allow the possibility of creep recovery and also the practical convenience of utilizing simple relaxation theory to predict total creep strain as a function of time, temperature and stress.

Thermal pretreatment of the CVD fibre at temperatures greater than 1400° C was observed to significantly increase fibre creep resistance, suggesting that some loss of free silicon may have occurred. Although this may appear to be a practical means for improving high-temperature deformation behaviour, these thermal treatments have also been observed to cause a measurable loss in fibre tensile strength. In a like manner, for CVD temperatures greater than 1300° C where the likelihood of free silicon formation is reduced, the fibre manufacturer has found less than optimum tensile strength for the as-produced fibres. These results suggest that although the free silicon may be somewhat detrimental to fibre creep deformation, its presence may be unavoidable if one desires high fibre tensile strength, a property of prime importance for the structural performance of ceramic composites. Indeed, the fundamental question arises whether excess silicon may in fact be a requirement for high fibre strength.

References

1. R. W. RICE, *Ceram. Eng. Sci. Proc.* **2** (1981) 661.
2. S. YAJIMA, *Amer. Ceram. Soc. Bull.* **62** (1983) 893.
3. H. DEBOLT and V. KRUKONIS, "Improvement of Manufacturing Methods for the Production of Low Cost Silicon Carbide Filament, "Air Force Contract F33615–72–C–1177, Report No. AFML–TR–73–140 (1973).
4. F. W. WAWNER, A. Y. TENG and S. R. NUTT, *Soc. Adv. Mater. Process Eng. Q.* **14** (1983) 39.
5. J. R. WEISS and R. J. DIEFENDORF, "Chemical Vapor Deposition", edited by G. Wakefield and J. M. Blocher, Jr (Electrochemical Society, Princeton, New Jersey, 1973) p. 488.
6. P. MARTINEAU, M. LAHAYE, R. PAILLER, R. NASLAIN, M. COUZI and F. CREUGE, *J. Mater. Sci.* **19** (1984) 2731.
7. J. A. CORNIE, R. J. SUPLINSKAS and A. W. HAUZE, *Ceram. Eng. Sci. Proc.* **1** (1980) 728.
8. R. J. SUPLINSKAS and H. DEBOLT, "Surface Enhancement of Silicon Carbide Filamant for Metal Matrix Composites," ONR Contract N00014–79–C–0691, AD–A110780 (1981).
9. R. T. BHATT, *J. Mater. Sci.* in press.
10. J. A. DICARLO and T. C. WAGNER, *Ceram. Eng. Sci. Proc.* **2** (1981) 872.
11. E. A. GULBRANSEN and S. A. JANSSON, *Oxid. Met.* **4** (1972) 3.
12. A. S. NOWICK and B. S. BERRY, "Anelastic Relaxation in Crystalline Solids" (Academic Press, New York, 1972).
13. E. L. KERN, D. W. HAMILL, H. W. DIEM and H. D. SHEETS, *Mater. Res. Bull.* **4** (1969) S25.
14. R. A. LOGAN and W. L. BOND, *J. Appl. Phys.* **30** (1959) 322.
15. J. A. DICARLO and W. WILLIAMS, *Ceram. Eng. Sci. Proc.* **1** (1980) 671.
16. P. L. FARNSWORTH and R. L. COBLE, *J. Amer. Ceram. Soc.* **49** (5) (1966) 264.
17. C. ZENER, *Phys. Rev.* **60** (1941) 906.
18. M. H. HON, R. F. DAVIS and D. E. NEWBURY, *J. Mater. Sci.* **15** (1980) 2073.
19. C. J. SMITHELLS and E. A. BRANDES, (editors), "Metals Reference Book", 5th edn. (Butterworths, London, 1976) p. 868.
20. P. MARSHALL and R. B. JONES, *Powder Metall.* **12** (23) (1969) 193.
21. D. C. LARSEN and J. W. ADAMS, "Properties Screening and Evaluation of Ceramic Turbine Materials," Air Force Cotnract F333615–79–C–5100, Report No. AFWAL–TR–83–4141 (1984).
22. G. SIMON and A. R. BUNSELL, *J. Mater. Sci. Lett.* **2** (1983) 80.
23. I. AHMAD, D. N. HILL, J. BARRANCO, R. WARENCHAK and W. HEFFERNAN, "Advanced Fibres and Composites for Elevated Temperatures", edited by I. Ahmad and B. R. Norton (Metallurgical Society of AIME, Warrendale, Pennsylvania, 1980) p. 156.

Received 14 January
and accepted 25 February 1985